Science of the Total Environment xxx (2016) xxx–xxx

Contents lists available at ScienceDirect

Science of the Total Environment

journal homepage: www.elsevier.com/locate/scitotenv

Validation of integrated water vapor from OMI satellite instrument against reference GPS data at the Iberian Peninsula

Javier Vaquero-Martínez[a,b,*], Manuel Antón[a,b], José Pablo Ortiz de Galisteo[c,d], Victoria E. Cachorro[d], Huiqun Wang[e], Gonzalo González Abad[e], Roberto Román[f,h], Maria João Costa[g]

[a] Departamento de Física, Universidad de Extremadura, Badajoz, Spain
[b] Instituto Universitario de Investigación del Agua, Cambio Climático y Sostenibilidad (IACYS), Universidad de Extremadura, Badajoz, Spain
[c] Agencia Estatal de Meteorología (AEMET), Valladolid, Spain
[d] Grupo de Óptica Atmosférica, Universidad de Valladolid, Valladolid, Spain
[e] Smithsonian Astrophysical Observatory, Cambridge, MA, United States
[f] Departamento de Física Aplicada, Universidad de Granada, Granada, Spain
[g] Departamento de Física, Instituto de Ciências da Terra, Escola de Ciências e Tecnología, Universidade de Évora, Évora, Portugal
[h] Andalusian Institute for Earth System Research (IISTA-CEAMA), University of Granada, Autonomous Government of Andalusia, 18006, Granada, Spain

HIGHLIGHTS

- Version 1.0 OMI IWV product is promising, in fairly good agreement with GPS data.
- OMI data can sometimes be unrepresentative to possible extreme local IWV values.
- Low IWV data show great variability (~ 100%) and overestimation (~ +40%).
- High IWV data show less variability and underestimation (~−20%).
- Seasonal and SZA dependence of OMI-GPS differences is mainly related to IWV.

GRAPHICAL ABSTRACT

ARTICLE INFO

Article history:
Received 14 October 2016
Received in revised form 3 December 2016
Accepted 4 December 2016
Available online xxxx

Editor: D. Barcelo

Keywords:
OMI
Water vapor
Validation
IWV
GPS
Satellite

ABSTRACT

This paper shows the validation of integrated water vapor (IWV) measurements retrieved from the Ozone Monitoring Instrument (OMI), using as reference nine ground-based GPS stations in the Iberian Peninsula. The study period covers from 2007 to 2009. The influence of two factors, - solar zenith angle (SZA) and IWV -, on OMI-GPS differences was studied in detail, as well as the seasonal dependence. The pseudomedian of the relative differences is $-1 \pm 1\%$ and the inter-quartile range (IQR) is 41%. Linear regressions calculated over each station show an acceptable agreement (R^2 up to 0.77). The OMI-GPS differences display a clear dependence on IWV values. Hence, OMI substantially overestimates the lower IWV data recorded by GPS (~40%), while underestimates the higher IWV reference values (~20%). In connection to this IWV dependence, the relative differences also show an evident SZA dependence when the whole range of IWV values are analyzed (OMI overestimates for high SZA values while underestimates for low values). Finally, the seasonal variation of the OMI-GPS differences is also associated with the strong IWV dependence found in this validation exercise.

* Corresponding author at: Departamento de Física, Universidad de Extremadura, Badajoz, Spain.
E-mail address: javier_vm@unex.es (J. Vaquero-Martínez).

http://dx.doi.org/10.1016/j.scitotenv.2016.12.032
0048-9697/

1. Introduction

Water vapor is the most important greenhouse gas on Earth, and plays a key role in the hydrological cycle (Myhre et al., 2013). Additionally, it provides latent heating when it condenses, and, according to general circulation models (Colman, 2003), it represents a positive climate feedback.

However, water vapor is also one of the most variable gases in the troposphere, both spatially and temporally (Myhre et al., 2013; Ortiz de Galisteo et al., 2011, 2014). Therefore, in order to assess climate change, knowledge of the spatio-temporal distribution of water vapor is fundamental. Since ground-based observations cannot provide a uniform global coverage (being specially scarce over polar and oceanic regions), it is necessary to use satellite measurements to improve spatial cover.

Water vapor is usually quantified using the column-integrated amount of atmospheric water vapor (IWV), equivalent to condensing all the water vapor in the atmospheric column and measuring the height that it would reach in a vessel of unit cross section; it can be measured in superficial density (g/mm^2) or in length (height) units (mm).

Over the years, multiple remote-sensing techniques have been developed to measure IWV both from ground sites and from space platforms. Among them, we find microwave radiometers (Jones et al., 2009; Turner et al., 2007), sun-photometers (Ichoku et al., 2002), Lidar (Turner et al., 2002), satellite measurements (Bennouna et al., 2013; Román et al., 2015; Wang et al., 2014), Global Positioning System (GPS) (Ortiz de Galisteo et al., 2011) and radiosounding (Jakobson et al., 2005; Torres et al., 2010).

Among ground-based water vapor instruments, GPS receiver stations are one of the most powerful techniques to measure IWV. It has been widely studied, as in Pany et al. (2001) and De Haan et al. (2002) (tested against a numerical model), and Ortiz de Galisteo et al. (2010) (for GPS antenna corrections). One of its main advantages is the independence of meteorological events, such as cloudiness or precipitation, along with the possibility of high temporal resolution (up to a few minutes) and low cost of the receivers, allowing a dense coverage (Köpken, 2001).

Unfortunately, ground-based measurements cannot resolve the spatial structures of global water vapor fields, and coverage is restricted mainly to land areas. Satellite observations are more suitable for weather forecasts and climate studies, due to high accuracy and high spatial resolution of IWV products. There are, however, two major drawbacks in polar orbiting satellite observations (Diedrich et al., 2016). First, most areas are sampled only once per day (or even less), depending on latitude and swath width of the instruments. Secondly, clouds are opaque in the visible and NIR spectra and therefore satellite IWV data under cloudy conditions are not reliable. Therefore, to reassure the quality of the IWV data derived from satellite instruments, validation exercises using reference measurements are required.

Numerous satellite instruments provide IWV data which have been widely inter-compared against reference ground-based measurements, namely, Global Ozone Monitoring Experiment-2 (GOME-2) (Grossi et al., 2015; Kalakoski et al., 2016; Noël et al., 2008; Román et al., 2015), MODerate-resolution Imaging Spectroradiometer (MODIS) (Bennouna et al., 2013; Chang et al., 2015; Gao and Li, 2008; Li et al., 2003; Ningombam et al., 2016; Prasad and Singh, 2009; Román et al., 2014), Meteosat (Hanssen et al., 2001; Schroedter-Homscheidt et al., 2008), MEdium Resolution Imaging Spectrometer (MERIS) (Diedrich et al., 2016; Li et al., 2006) or SCIAMACHY (Bovensmann et al., 1999; Noël et al., 2005; Schrijver et al., 2009). Additionally, the Ozone Monitoring Instrument (OMI) also provides IWV data using the retrieval algorithm proposed by Wang et al. (2014). However, to our knowledge, only one validation exercise using the IWV product from OMI can be found in literature (Wang et al., 2016) and that paper presented comparisons on a global scale using reference data that are different from those used in the present work.

This paper focuses on the validation of the IWV data obtained from the OMI satellite instrument using as reference the GPS IWV data recorded at nine stations in the Iberian Peninsula, covering the period 2007–2009. The main objective of this paper is to quantify the differences between IWV obtained from OMI and GPS, considered as reference, in order to improve the understanding of the quality and accuracy of the OMI IWV data.

The paper is organized as follows. Datasets are described in Section 2. Section 3 shows the methodology to carry out the study. Results are presented in Section 4, and, finally, conclusions are drawn in Section 5.

2. Data

2.1. OMI data

OMI (Levelt et al., 2006) was launched on 15 of July 2004 onboard NASA Earth Observing System (EOS) Aura satellite into a Sun-synchronous polar orbit. Developed by the Netherland's Agency for Aerospace Programs (NIVR) and the Finnish Meteorological Institute (FMI), OMI UV/Vis spectrograph samples the whole planet daily at 1330 local time (LT).

The OMI IWV data used in this study are the first version of Smithsonian Astrophysical Observatory (SAO) OMH2O level 2 retrievals which uses the SAO operational retrieval algorithm presented in detail in González Abad et al. (2015).

The visible channel (349 nm –504 nm) of OMI covers several water vapor spectral bands. These bands are weak compared with bands at longer wavelengths. Using the 7ν and $6\nu + \delta$ polyads between 430 –480 nm helps to avoid non-linearity due to saturation. Another feature that makes this retrieval valuable and unique among satellite retrievals is the more uniform albedo over the globe making results over land and water consistent. Despite albedo uniformity, validation analysis carried on by Wang et al. (2016), showed a significant bias (around 5% lower) of SAO OMH2O version 1 compared to in-situ measurements over the oceans.

The retrieval follows these steps: (1) direct fitting of Slant Column Density (SCD) using a semi-empirical model considering several gases (water vapor, ozone, nitrogen dioxide, O_2-O_2, glyxoal, liquid water), the Ring effect, the water Ring effect, 3rd order closure polynomials, wavelength shift, under-sampling correction, and common mode. (2) SCD conversion to Vertical Column Density (VCD) by dividing SCD by the Air Mass factor (AMF). AMF are calculated using radiative transfer calculations saved in look-up-tables (LUT) at 442 nm. LUTs are dependent on viewing geometry (solar zenith angle (SZA), viewing zenith angle (VZA) and relative azimuth angle (RAA)) and surface properties (pressure and albedo). It is important here to mention that AMF is notably sensitive to cloudiness (Wang et al., 2016). Finally, VCD can be converted easily to IWV multiplying by a factor (molecular weight of water divided by Avogadro constant). A full description of the retrieval set up can be found in Wang et al. (2014).

Following the guidelines provided by Wang et al. (2014) for OMH2O quality the cloud fraction had to be lower than 0.1, cloud top pressure greater than 500 HPa, air mass factor greater than 0.75 and retrieval root mean square (RMS) value for the fitting Slant Column Density lower than 0.005. Moreover, only pixel whose *maindataqualityflag* flag were equal to 0 were chosen, and pixels affected by the row anomaly (Wang et al., 2014) have been rejected as well.

2.2. GPS data

GPS IWV data used in this work were derived from ground-based GPS measurements of zenith total delay (ZTD) using tropospheric

Please cite this article as: J. Vaquero-Martínez et al., Validation of integrated water vapor from OMI satellite instrument against reference GPS data at the Iberian Peninsula, Science of the Total Environment (2016), http://dx.doi.org/10.1016/j.scitotenv.2016.12.032

products from Spanish Geographic Institute "Instituto Geográfico Nacional", a local analysis center of the European Reference Frame (EUREF). These GPS data have been successfully used to perform exhaustive validation exercises on satellite IWV data derived from GOME-2 (Román et al., 2015), and MODIS (Bennouna et al., 2013). The IWV retrieval from GPS method is thoroughly explained in Bevis et al. (1992). In the present paper, a brief description is provided.

GPS consists of a constellation of satellites that communicate through microwave with ground-based receivers. The time that the microwave signal spends on reaching the receiver is used to calculate the distance from the receiver to the satellites. Several corrections must be made (relativistic corrections, ionospheric delay, and so on). The effect of troposphere can be accounted for in the Slant Tropospheric Delay (STD), which can be converted through the so-called mapping functions Niell (2000) to Zenith Tropospheric Delay (ZTD). After calculating ZTD with GPS measurements, it can be divided into the sum of two contributions: Zenith Hydrostatic Delay (ZHD), due to tropospheric gases, and Zenith Wet Delay (ZWD) due to water vapor. ZHD can be modeled and removed by knowing the surface atmospheric pressure and temperature at station level. Thus, ZWD can be calculated and converted to IWV.

In order to estimate the hydrostatic contribution of the delay, two variables are needed, temperature and pressure at the location of GPS station, which are provided by the Spanish Meteorological State Agency (AEMET). It must be noted that these meteorological stations are not in the same place as GPS stations, but elsewhere in the same town or very close to each other, as well as not measuring at the same times. Thus, interpolation is needed. Temperature measurement data are interpolated linearly to the time of GPS measurements. For pressure interpolation the barometric tide was taken into account. Such effect has an amplitude of about 0.5 mb, but GPS IWV observations are quite sensitive to uncertainties in pressure (Hagemann et al., 2003). Moreover, the diurnal IWV cycle is quite low. Hence, if a linear interpolation were used for pressure, part of pressure's diurnal cycle would be transferred to IWV's cycle. Furthermore, a correction based on the difference of altitude between GPS and meteorological stations was made, considering a standard atmosphere with a vertical gradient of temperature of 6.5 °C/km (Ortiz de Galisteo et al., 2014). The IWV data at the nine GPS stations are available for the period 2007–2009.

The GPS dataset has a temporal resolution of an hour. Nine GPS stations in the interior of the Iberian Peninsula were chosen, in order to avoid introducing data that might be influenced by sea or mixed sea-land pixels in the satellite observations. A summary of the stations and their IWV characteristics can be found in Table 1, along with a map showing their locations in Fig. 1. In Table 1, the median and IQR of the GPS IWV of every station is shown. *coba* station has the highest median (16.29 mm), while *leon* has the lowest median (9.27 mm). The rest of stations have medians of 11–13 mm except for *rioj*, which has a median of 14.89 mm. The IQR show higher variability in *rioj* station (11.90), while *leon* has the lowest IQR (7.55). The IQR of the rest of stations are between 8 and 10 mm.

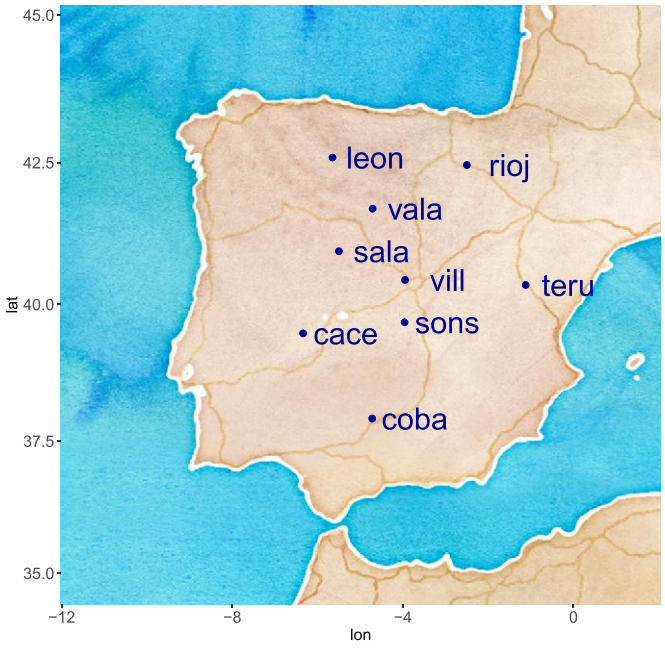

Fig. 1. Location of the nine stations selected.

3. Methodology

3.1. Comparison criteria

The spatial co-location between GPS and OMI follows these criteria: OMI pixels have to have their center within 0.25° longitude and 0.25° latitude distance to the GPS station. If there is more than one pixel, the average is calculated, weighted by the fitting error.

Regarding temporal co-location, OMI collects data over the Iberian Peninsula at 13.30 h (LT) every day. Thus, GPS data selected to match OMI data is always at 13.30 h, without any delay between both instruments measurements. Data with very high uncertainties (σ(ZTD) > 1.5 mm for GPS and ΔIWV_{OMI} > 10 mm for OMI) have been rejected.

Table 1
Location and statistics of IWV at the GPS stations considered. The Median and IQR columns show the median and IQR of IWV obtained by GPS. All stations include data from Start date (last column) to 12/31/09.

Station	Acronym	Latitude (°)	Longitude (°)	Altitude (m)	N	Median (mm)	IQR (mm)	Start date mm/dd/yy
Córdoba	coba	37.92	−4.72	162	605	16.3	9.2	01/01/07
León	leon	42.59	−5.65	915	390	9.3	7.6	09/09/07
Logroño	rioj	42.46	−2.5	452	365	14.9	11.9	01/21/07
Salamanca	sala	40.95	−5.5	800	524	11.4	8.0	01/01/07
Sonseca	sons	39.68	−3.96	755	429	11.1	9.2	09/09/07
Teruel	teru	40.35	−1.12	956	188	11.7	9.7	09/28/08
Valladolid	vala	41.70	−4.71	766	264	12.6	8.3	04/20/08
Villafranca	vill	40.44	−3.95	596	532	12.8	9.2	01/01/07
Cáceres	cace	39.48	−6.34	384	598	12.8	8.8	01/01/07
All	All	–	–	–	3895	12.8	9.2	–

Please cite this article as: J. Vaquero-Martínez et al., Validation of integrated water vapor from OMI satellite instrument against reference GPS data at the Iberian Peninsula, Science of the Total Environment (2016), http://dx.doi.org/10.1016/j.scitotenv.2016.12.032

3.2. Statistical analysis

The study is carried out by building a dataset where every row has an OMI datum, a GPS datum, the station, and additional information, such as Solar Zenith Angle (SZA), date, and so on. The GPS and OMI data are matched according to the spatial and temporal criteria mentioned in the previous section. The relative differences (δ) are analyzed. The relative difference is calculated as:

$$\delta_i = 100 \cdot \frac{w_i^{\mathrm{OMI}} - w_i^{\mathrm{GPS}}}{w_i^{\mathrm{GPS}}}$$

where the index i denotes a certain location and date, w is the IWV measured by OMI or GPS. In order to study the distribution of δ, two indices are applied: the pseudomedian ($\bar{\delta}$) and the interquartile range (IQR). The pseudomedian is calculated through Wilcoxon signed rank test with continuity correction (Wilcoxon, 1946). The pseudomedian agrees with the median (the datum that has as many data over it as under it) in a symmetric dataset. It is defined as the median of all the midpoints of pairs of observations. The pseudomedian gives a measurement of the accuracy. If it was close to zero, OMI and GPS would be very close, but if it was positive, it would mean that OMI is overestimating IWV, while a negative value of the pseudomedian would be a sign of an underestimation tendency of OMI data. IQR is the difference between the first (the datum that has 25% of data under it and 75% over it) and the third (the datum that has 75% of data under it and 25% over it) quartile. This gives the width of the central half of the data, being therefore a measurement of the precision of the satellite measurement.

In this context, a statistical analysis per station has been performed, in order to detect differences between stations. In the analysis, indices over each station have been calculated, and a linear regression analysis between the GPS and the OMI data is performed for each ground-based GPS station and for all stations together in order to analyze their proportionality and similarity. In order to study the influence of other parameters (SZA, IWV and season) on these indices, data have been binned for these variables. The indices calculated over the binned data have been plotted against the central value of the bin. For IWV, the bin width was 5 mm, for SZA 5° and for seasonal dependence, one month. Bins with less than 30 data are ignored in this paper.

4. Results and discussion

4.1. Statistical analysis

A statistical analysis was performed on the nine stations. Table 2 shows the results of this analysis, where the pseudomedian and IQR of the δ distribution are calculated, and a regression analysis is performed between OMI and GPS IWV data. The pseudomedian values show that OMI both underestimates and overestimates the reference GPS data, with values between −19% for *rioj* and +23% for *teru*. The values of pseudomedian and IQR have been also calculated in absolute value (in mm), reporting values of −2.8 mm (*rioj*) and +2.5 mm (*teru*) for the pseudomedian, and around 4 mm for the IQR

This over/under-estimation shown in the signs of the pseudomedian values in Table 2 can be partially related to the IWV distribution at each ground-based station. In order to clarify this issue, the histogram of the station with highest overestimation (*teru*) and underestimation (*rioj*) is shown in Fig. 2. In this plot, it can be appreciated that *teru* tends to have lower IWV than *rioj*, where higher IWV values are more common. This suggests that those stations with low values of IWV tend to be overestimated by OMI, while those with higher values of IWV tend to be underestimated. This IWV dependence will be analyzed in detail in the next subsection. Another reason for the differences between stations could be their altitude, since the AMF correction is affected by this variable (Palmer et al., 2001). From our results, most ground-based stations located at higher altitude show greater IQR and pseudomedian values than the stations at lower altitude.

The all-stations row shows that, on average, OMI observations slightly underestimate the reference GPS data (~1%), which is in good agreement with the results reported by Wang et al. (2016). IQR ranges approximately between 30% and 50%, with a value of 41% when all data are analyzed together. Part of the variability is related to the stripes in OMI data which can be up to 15–20% (Wang et al., 2014). Nevertheless, the high IQR values in Table 2 indicate a notable variability in the OMI-GPS relative differences over the study region.

The slopes derived from the linear regression analysis are around 0.8 while the intercepts are generally positive, suggesting that data tend to be overestimated for lower values of IWV and underestimated for the higher ones. In order to show this more clearly, Fig. 3 shows the scatter-plot between OMI and GPS using all data from the nine stations. The regression line is above the 1:1 line when IWV is lower than ~12 mm. The R^2 values are between 0.6 and 0.7 in most stations which indicates a fairly good agreement between OMI and GPS data.

In Fig. 4, time series plots are shown for each station. As shown in Table 1, some GPS stations started working after 01/01/2007. GPS and OMI appear to agree reasonably well. Stations *coba*, *rioj* and *vala* show a trend towards negative OMI-GPS differences, while *sala*, *sons* and *teru* are prone to positive OMI-GPS differences. The rest of stations do not show a clear behavior.

4.2. IWV dependence

The OMI-GPS differences display an evident dependence on IWV values as can be observed in Fig. 5 (top). In this plot, the pseudomedians of relative differences are represented against IWV in bins of

Table 2
Statistical analysis of OMI-GPS relative differences. The pseudomedian (pMedian) and IQR of the δ distribution, the number of data (N) and the coefficients of the regression analysis are shown. y_0 column shows the intercept, b stands for the slope and R^2 is Pearson's coefficient of determination. The numbers in parenthesis are the 95% confidence interval.

Station	pMedian (mm)	IQR (mm)	pMedian (%)	IQR (%)	N	y_0 (mm)	b	R^2
coba	−2.3(0.3)	5.0	−13(2)	27.5	605	1.7(0.8)	0.76(0.04)	0.67
leon	−0.7(0.4)	4.9	−5(4)	51.6	390	1.8(0.9)	0.77(0.08)	0.51
rioj	−2.8(0.3)	4.3	−19(2)	26.7	365	−0.3(0.8)	0.84(0.05)	0.77
sala	1.4(0.3)	4.9	15(3)	48.4	524	3.1(0.7)	0.86(0.06)	0.64
sons	1.6(0.3)	3.9	18(3)	41.3	429	3.4(0.7)	0.85(0.05)	0.71
teru	2.5(0.6)	4.6	23(6)	43.1	188	3.2(1.3)	0.96(0.09)	0.69
vala	−0.8(0.4)	3.6	−5(3)	29.8	264	2.2(0.9)	0.78(0.06)	0.68
vill	−0.7(0.3)	4.5	−4(3)	35.7	532	2.4(0.7)	0.78(0.05)	0.66
cace	−0.1(0.3)	4.7	0(3)	37.4	598	2.3(0.8)	0.84(0.05)	0.63
All	−0.3(0.1)	5.1	−1(1)	40.8	3895	2.7(0.3)	0.78(0.02)	0.63

Please cite this article as: J. Vaquero-Martínez et al., Validation of integrated water vapor from OMI satellite instrument against reference GPS data at the Iberian Peninsula, Science of the Total Environment (2016), http://dx.doi.org/10.1016/j.scitotenv.2016.12.032

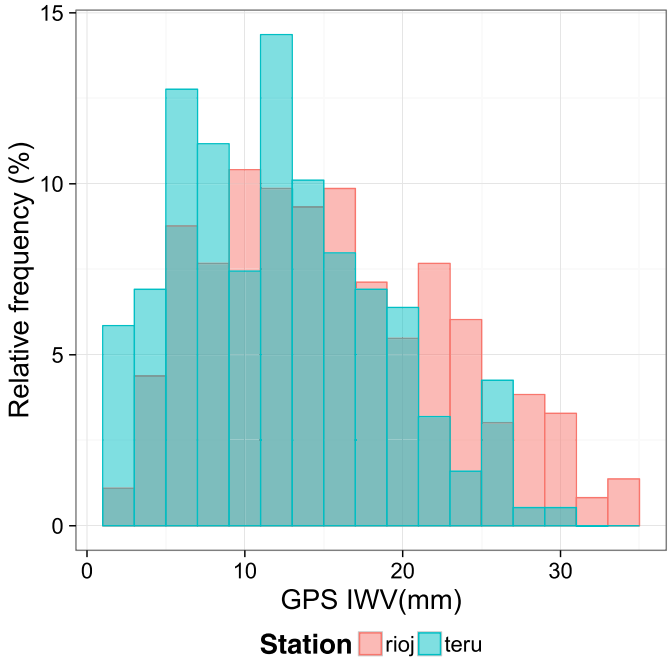

Fig. 2. Histogram of IWV values (GPS) for the stations *teru* and *rioj*.

5 mm. The error bars are the 95% confidence interval in the Wilcoxon signed rank test with continuity correction. A strong overestimation (40%) is observed for low IWV values. By contrast, high IWV values tend to be underestimated (about 15%). Additionally, the OMI-GPS differences corresponding to intermediate IWV values, around 10–15 mm are the closest to 0. This IWV dependence can be probably related to the fact that the IWV is averaged over the closest pixels at 0.25° latitude × 0.25° longitude neighborhood pixels, while GPS provides the local value. As a consequence, if a ground-based station exhibits an extreme value of IWV (very low or very high) compared with the area nearby the average OMI IWV will tend to overestimate low IWV and underestimate high IWV. Moreover, two subsets are also plotted in Fig. 5: high (above 40°) and low (below 40°) SZA values. The behavior is not significantly different between them, which points out that the OMI-GPS dependence on IWV does not depend on the SZA range selected for the analysis.

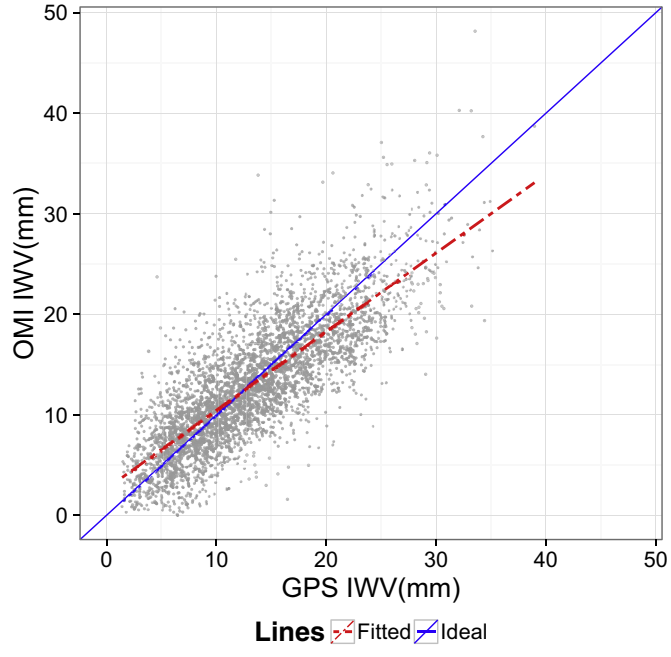

Fig. 3. Scatter-plot of OMI IWV vs. GPS IWV. The red, dashed line is the linear regression and the black, solid line is the 1:1 line. (For interpretation of the references to color in this figure legend, the reader is referred to the web version of this article.)

Fig. 5 (bottom) shows the influence of IWV over the IQR derived from the OMI-GPS relative differences. There is a sharp decrease of IQR with increasing IWV, with OMI-GPS differences greatly disperse (over 100%) for IWV values below 5 mm and less than 20% for IWV above 20 mm. Additionally, the difference between high and low SZA is very little, with the values for low SZA slightly lower than those for high SZA.

4.3. SZA dependence

The influence of SZA on the satellite instruments performance has been reported in Antón et al. (2015) and Román et al. (2015) for GOME-2, which uses a window in the visible part of the spectrum like OMI. Fig. 6 (top) shows a strong dependence of pseudomedian IWV values on SZA when the whole range of IWV values is used in the analysis. For low SZA (below 35°), OMI underestimates the GPS IWV data. This pattern is the opposite when dealing with high SZA, being the pseudomedian of differences positive and uncertainty higher. The best agreement between both instruments is achieved for intermediate SZAs ($35° < SZA < 60°$). However, if a distinction is made between low (below 12.75 mm) and high IWV (above 12.75 mm), there is a clear difference in the behavior of these two subsets with respect to the whole dataset. Low IWV values are notably overestimated, while high IWV data are underestimated, in agreement with the results shown in the previous section. Moreover, the pseudomedian of both subsets does not significantly change with SZA, suggesting that the SZA dependence observed for the whole dataset can be associated with the seasonal cycle of IWV data over the study region with the smallest IWV values in winter (high SZA) and the largest in summer (low SZA). In fact, at low SZA, temperatures are higher, and more water vapor can be accepted by the atmosphere. However, at higher SZA, temperatures are lower, and not so much water vapor can be accepted by the atmosphere.

IQR, however, is clearly lower for low SZA (less than 30%) than for high SZA (75%), as it can be observed in Fig. 6 (bottom). There is an increasing tendency of IQR with SZA. Nevertheless, high IWV data have IQR values between 25% and 30% for all SZA, while low IWV data have a larger variation with SZA. The values of IQR for the whole dataset seem to be heavily influenced by the value of IWV.

4.4. Seasonal dependence

Fig. 7 (top) shows a clear seasonal dependence of the OMI-GPS differences due to the fact that conditions of humidity (IWV) differ from one season to another. Regarding all IWV conditions, summer months (June, July and August) are underestimated by OMI between a 5% and a 10%. Winter months (December, January and February) are, however, overestimated, with greater uncertainty. The months when OMI-GPS values are closer to zero are in the spring (March, April and May) and autumn (September, October and November), except for March (which behaves like winter months) and September (which behaves like summer months). This behavior is similar to the one reported in Wang et al. (2016). In Fig. 7 two subsets have been considered: low IWV and high IWV, with the values considered in Section 4.3. High IWV subsets do not change notably throughout the year, being underestimated. The low IWV subset is mostly overestimated.

IQR is shown in Fig. 7 (bottom). For all IWV conditions, Summer months have the lowest IQR (30%). Winter months have very high IQR, reaching 75% for December. Spring and autumn show

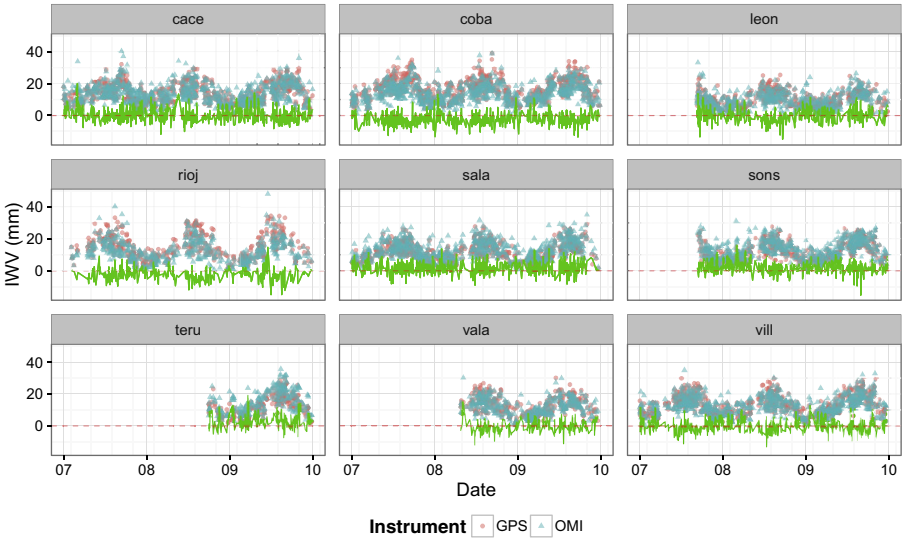

Fig. 4. Time series of IWV from both instruments, OMI and reference GPS, for each station . The green line shows the difference between OMI and GPS IWV measurements. The date is in years. (For interpretation of the references to color in this figure legend, the reader is referred to the web version of this article.)

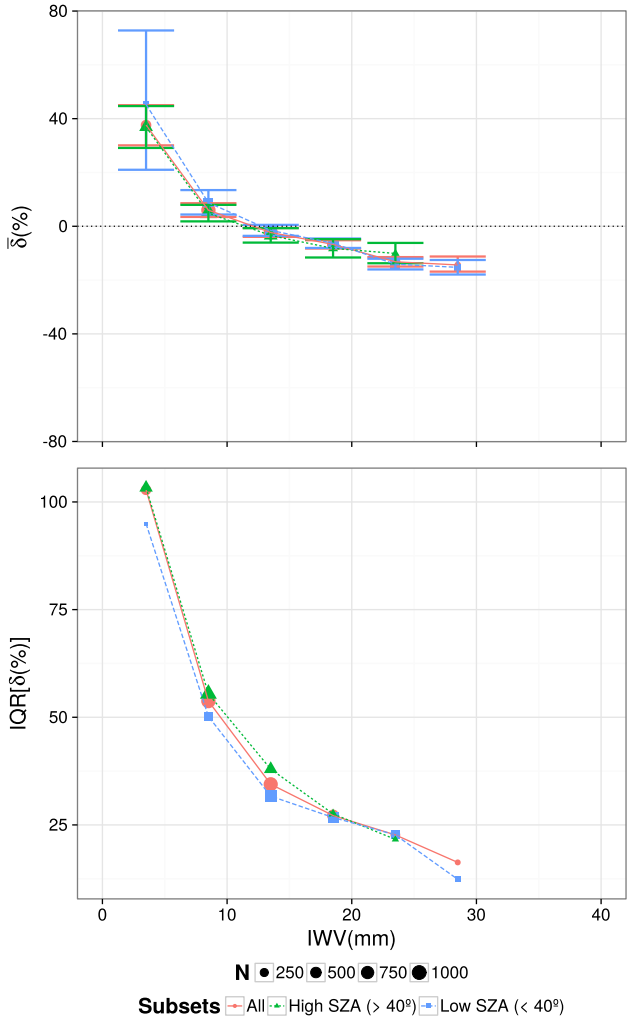

Fig. 5. IWV dependence on the pseudomedian (top) and the IQR (bottom) of OMI-GPS relative differences. The size of dots represents the number of data used to obtain the index for that data point (N).

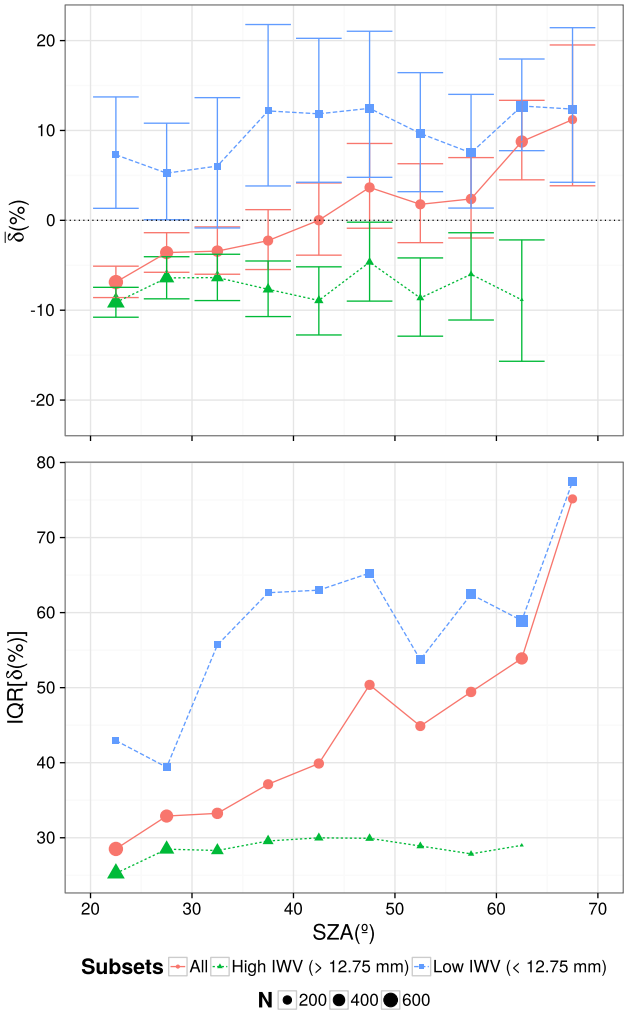

Fig. 6. SZA dependence on the pseudomedian (top) and the IQR (bottom) of OMI-GPS relative differences. The size of dots represents the number of data used to obtain the index for that data point (N).

Please cite this article as: J. Vaquero-Martínez et al., Validation of integrated water vapor from OMI satellite instrument against reference GPS data at the Iberian Peninsula, Science of the Total Environment (2016), http://dx.doi.org/10.1016/j.scitotenv.2016.12.032

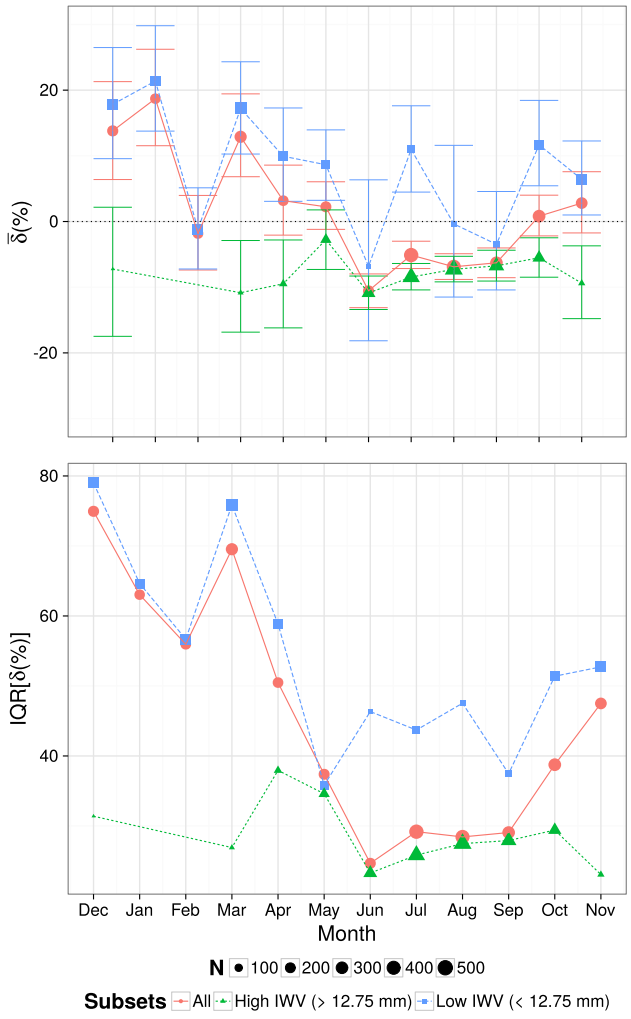

Fig. 7. Seasonal dependence on the pseudomedian (top) and IQR (bottom) of OMI-GPS relative differences. The size of dots represents the number of data used to obtain the index for that data point (N). December has been rearranged as the first month in order to facilitate the identification of the different seasons.

intermediate performance. Regarding the subsets studied, the low IWV subset has clearly higher IQR than the high IWV subset. This pattern is very different from the one reported in Wang et al. (2016), where the index used was the standard deviation of the differences OMI-GPS (in mm), and summer months have larger differences than winter months. One reason for this could be the fact that during summer months IWV is higher, and thus the relative differences are low in percentage. In winter, the opposite happens: IWV is low, making small absolute differences appear large in terms of percentage. It is worth noticing that the standard deviation reported by Wang et al. (2016) ranges from 5 mm to 7 mm, while IWV ranges from 1 mm to 39 mm. It can be observed that low IWV subset presents lower IQR that high IWV throughout the year, and that the decrease in summer months of IQR for all IWV conditions is due to larger amount of high IWV cases than low IWV cases.

5. Conclusions

The period 2007 –2009 has been studied to validate the IWV data retrieved by OMI against the GPS reference data at nine land ground-based stations in the Iberian Peninsula. The IWV values retrieved from OMI show a strong dependence on IWV values. Satellite IWV data tend to overestimate (pseudomedian values around 40%) low IWV data, showing high variability. For high IWV data, the behavior is the opposite: OMI underestimates the reference GPS data (pseudomedian value around 20%) and the variability is lower. The over/under-estimation can be partially related to OMI – GPS data co-location: OMI data is averaged using the pixels in the neighborhood of GPS station. Additionally, satellite IWV data are retrieved using albedo, surface pressure and other information. This is in contrast to the local nature of GPS measurement. Consequently, OMI measurements can sometimes be unrepresentative to possible extreme local IWV values.

The effect of SZA on the water vapor column retrieved by OMI satellite instrument is highly dependent on the seasonal cycle of IWV values over the study region, with the highest IWV values in summer and the lowest in winter. Thus, low SZA data has similar accuracy and precision as high IWV data. Low SZA data tend to be underestimated and have less variability. High SZA, however, is related to low IWV values, which leads to overestimation and high variability. The little impact of SZA on OMI-GPS IWV differences contrast with Román et al. (2015), where a strong dependence of SZA on the differences between GOME-2 IWV and GPS in the Iberian Peninsula was found. This points out that OMI retrieval appears to be more independent of SZA values than GOME-2 retrieval.

The seasonal variation found for the OMI–GPS differences is mainly related to IWV. Summer months have high IWV values (higher temperatures), exhibiting underestimation and low variability, while winter months are associated with low IWV (low temperatures), with overestimation and high variability. Even in the best cases of OMI-GPS agreement, the IQR is high (more than 25%) which suggests increase variability of the relative differences.

In summary, although the version 1.0 OMI satellite water vapor product is very promising, in a fairly good agreement with reference GPS data, it still needs improvements in order to reduce the variability and IWV dependence. An updated version 2.1 OMI algorithm shows the potential to improve data quality, as reported in Wang et al. (2016). Its performance should be tested once the data is released.

Acknowledgements

This work was supported by the Spanish Ministry of Economy and Competitiveness through project CGL2014-56255-C2. Manuel Antón thanks Ministerio de Ciencia e Innovación and Fondo Social Europeo (RYC-2011-08345) for the award of a postdoctoral grant (Ramón y Cajal). Support from the Junta de Extremadura (Research Group Grants GR15137) is gratefully acknowledged. Work at Universidad de Valladolid is supported by project CMT2015-66742-R. Work at Universidad de Granada was supported by the Andalusia Regional Government (project P12-RNM-2409) and the Spanish Ministry of Economy and Competitiveness and FEDER funds under the projects CGL2013-45410-R and "Juan de la Cierva-Formación" program. Work at SAO is supported by NASA's Atmospheric Composition: Aura Science Team program (sponsor contract number NNX14AF56G). Work at Universidade de Évora is co-funded by the European Union through the European Regional Development Fund, included in the COMPETE 2020 (Operational Program Competitiveness and Internationalization) through the ICT project (UID/GEO/04683/2013) with the reference POCI-01-0145-FEDER-007690.

References

Antón, M., Loyola, D., Román, R., Vömel, H., 2015. Validation of GOME-2/MetOp-A total water vapour column using reference radiosonde data from the GRUAN network. Atmos. Meas. Tech. 8, 1135–1145. http://dx.doi.org/10.5194/amt-8-1135-2015.

Bennouna, Y.S., Torres, B., Cachorro, V.E., Ortiz de Galisteo, J.P., Toledano, C., 2013. The evaluation of the integrated water vapour annual cycle over the iberian peninsula from EOS-MODIS against different ground-based techniques. Q. J. Roy. Meteorol. Soc. 139, 1935–1956. http://dx.doi.org/10.1002/qj.2080.

Bevis, M., Businger, S., Herring, T. a., Rocken, C., Anthes, R. a., Ware, R.H., 1992. GPS meteorology: remote sensing of atmospheric water vapor using the global positioning system. J. Geophys. Res. 97, 15787–15801. http://doi.wiley.com/10.1029/92JD01517. http://dx.doi.org/10.1029/92JD01517.

Bovensmann, H., Burrows, J.P., Buchwitz, M., Frerick, J., Noël, S., Rozanov, V.V., Chance, K.V., Goede, a.P.H., 1999. SCIAMACHY: mission objectives and measurement modes. J. Atmos. Sci. 56, 127–150. http://dx.doi.org/10.1175/1520-0469(1999)056¡0127:SMOAMM¿2.0.CO;2.

Chang, L., Gao, G., Jin, S., He, X., Xiao, R., Guo, L., 2015. Calibration and evaluation of precipitable water vapor from MODIS infrared observations at night. IEEE Trans. Geosci. Remote Sens. 53, 2612–2620. http://dx.doi.org/10.1109/TGRS.2014.2363089.

Colman, R., 2003. A comparison of climate feedbacks in general circulation models. Climate Dynam. 20, 865–873. http://link.springer.com/article/10.1007/s00382-003-0310-z. http://dx.doi.org/10.1007/s00382-003-0310-z.

De Haan, S., Van Der Marel, H., Barlag, S., 2002. Comparison of GPS slant delay measurements to a numerical model: case study of a cold front passage. Phys. Chem. Earth 27, 317–322. http://dx.doi.org/10.1016/S1474-7065(02)00006-2.

Diedrich, H., Wittchen, F., Preusker, R., Fischer, J., 2016. Representativeness of total column water vapour retrievals from instruments on polar orbiting satellites. Atmos. Chem. Phys. Discuss. 16, 8331–8339. http://dx.doi.org/10.5194/acp-2016-99.

Gao, B.C., Li, R.R., 2008. The time series of terra and aqua MODIS near-IR water vapor products. Int. Geosci. Remote Sens. Symp. (IGARSS) 3, 186–189. http://dx.doi.org/10.1109/IGARSS.2008.4779314.

González Abad, G., Liu, X., Chance, K., Wang, H., Kurosu, T.P., Suleiman, R., 2015. Updated smithsonian astrophysical observatory ozone monitoring instrument (SAO OMI) formaldehyde retrieval. Atmos. Meas. Tech. 8, 19–32. http://dx.doi.org/10.5194/amt-8-19-2015.

Grossi, M., Valks, P., Loyola, D., Aberle, B., Slijkhuis, S., Wagner, T., Beirle, S., Lang, R., 2015. Total column water vapour measurements from GOME-2 metop-a and metop-b. Atmospheric Measurement Techniques 8, 1111–1133. http://www.atmos-meas-tech.net/8/1111/2015/.http://dx.doi.org/10.5194/amt-8-1111-2015.

Hagemann, S., Bengtsson, L., Gendt, G., 2003. On the determination of atmospheric water vapor from GPS measurements - art. no. 4678. J. Geophys. Res.-Atmos. 108, 4678.

Hanssen, R.F., Feijt, A.J., Klees, R., 2001. Comparison of precipitable water vapor observations by spaceborne radar interferometry and meteosat 6.7 – μm radiometry. J. Atmos. Ocean. Technol. 18, 756–764. http://dx.doi.org/10.1175/1520-0426(2001)058¡0756:COPWVO¿2.0.CO;2.

Ichoku, C., Levy, R., Kaufman, Y.J., Remer, L.A., Li, R.R., Martins, V.J., Holben, B.N., Abuhassan, N., Slutsker, I., Eck, T.F., Pietras, C., 2002. Analysis of the performance characteristics of the five-channel microtops II sun photometer for measuring aerosol optical thickness and precipitable water vapor. J. Geophys. Res. Atmos. 107, http://dx.doi.org/10.1029/2001JD001302.

Jakobson, E., Ohvril, H., Okulov, O., Laulainen, N., 2005, jun. Variability of radiosonde-observed precipitable water in the Baltic region. Nord. Hydrol. 36, 423–433.

Jones, A., Urban, J., Murtagh, D.P., Eriksson, P., Brohede, S., Haley, C., Degenstein, D., Bourassa, A., Von Savigny, C., Sonkaew, T., Rozanov, A., Bovensmann, H., Burrows, J., 2009. Evolution of stratospheric ozone and water vapour time series studied with satellite measurements. Atmos. Chem. Phys. Discuss 9, 1157–1209. www.atmos-chem-phys-discuss.net/9/1157/2009/. http://dx.doi.org/10.5194/acpd-9-1157-2009.

Kalakoski, N., Kujanpää, J., Sofieva, V., Tamminen, J., Grossi, M., Valks, P., 2016. Validation of GOME-2/MetOp total column water vapour with ground-based and in situ measurements. Atmos. Meas. Tech. 9, 1533–1544. http://dx.doi.org/10.5194/amt-9-1533-2016.

Köpken, C., 2001. Validation of integrated water vapor from numerical models using ground-based GPS, SSM/I, and water vapor radiometer measurements. J. Appl. Meteorol. 40, 1105–1117. http://dx.doi.org/10.1175/1520-0450(2001)040¡1105:VOIWVF¿2.0.CO;2.

Levelt, P.F., van den Oord, G.H.J., Dobber, M.R., Malkki, A., Visser, H., de Vries, J., Stammes, P., Lundell, J.O.V., Saari, H., 2006. The ozone monitoring instrument. IEEE Trans. Geosci. Remote Sens. 44, 1093–1101. http://dx.doi.org/10.1109/TGRS.2006.872333.

Li, Z., Muller, J., Cross, P., Albert, P., Fischer, J., Bennartz, R., 2006. Assessment of the potential of MERIS near-infrared water vapour products to correct ASAR interferometric measurements. Int. J. Remote Sens. 27, 349–365. http://dx.doi.org/10.1080/01431160500307342.

Li, Z., Muller, J.P., Cross, P., 2003. Comparison of precipitable water vapor derived from radiosonde, GPS, and moderate-resolution imaging spectroradiometer measurements. J. Geophys. Res. Atmos. 108, http://dx.doi.org/10.1029/2003JD003372.

Myhre, G., Shindell, D., Bréon, F.-M., Collins, W., Fuglestvedt, J., Huang, J., Koch, D., Lamarque, J.-F., Lee, D., Mendoza, B., Nakajima, T., Robock, A., Stephens, G., Takemura, T., Zhang, H., 2013, . Anthropogenic and natural radiative forcing. Technical Report WG1AR5. http://dx.doi.org/10.1017/CBO9781107415324.018.

Niell, A.E., 2000. Improved atmospheric mapping functions for VLBI and GPS. Earth Planets Space 52, 699–702. http://dx.doi.org/10.1186/BF03352267.

Ningombam, S.S., Jade, S., Shrungeshwara, T.S., Song, H.J., 2016. Validation of water vapor retrieval from moderate resolution imaging spectro-radiometer (MODIS) in near infrared channels using GPS data over IAO-Hanle, in the trans-himalayan region. J. Atmos. Sol. Terr. Phys. 137, 76–85. http://dx.doi.org/10.1016/j.jastp.2015.11.019.

Noël, S., Buchwitz, M., Bovensmann, H., Burrows, J.P., 2005. Validation of SCIAMACHY AMC-DOAS water vapour columns. Atmos. Chem. Phys. 5, 1835–1841. http://dx.doi.org/10.5194/acp-5-1835-2005.

Noël, S., Mieruch, S., Bovensmann, H., Burrows, J.P., 2008. Preliminary results of GOME-2 water vapour retrievals and first applications in polar regions. Atmos. Chem. Phys. 8, 1519–1529. http://dx.doi.org/10.5194/acp-8-1519-2008.

Ortiz de Galisteo, J.P., Bennouna, Y., Toledano, C., Cachorro, V., Romero, P., Andrés, M.I., Torres, B., 2014. Analysis of the annual cycle of the precipitable water vapour over Spain from 10-year homogenized series of GPS data. Q. J. Roy. Meteorol. Soc. 140, 397–406. http://dx.doi.org/10.1002/qj.2146.

Ortiz de Galisteo, J.P., Cachorro, V., Toledano, C., Torres, B., Laulainen, N., Bennouna, Y., de Frutos, A., 2011. Diurnal cycle of precipitable water vapor over Spain. Q. J. Roy. Meteorol. Soc. 137, 948–958. http://dx.doi.org/10.1002/qj.811.

Ortiz de Galisteo, J.P., Toledano, C., Cachorro, V., Torres, B., 2010. Improvement in PWV estimation from GPS due to the absolute calibration of antenna phase center variations. GPS Solutions 14, 389–395. http://dx.doi.org/10.1007/s10291-010-0163-y.

Palmer, P.I., Jacob, D.J., Chance, K., Martin, R.V., Spurr, R.J.D., Kurosu, P., Bey, I., Yantosca, R., Fiore, A., Li, Q., 2001. Air mass factor formulation for spectroscopic measurements from satellites: application to formaldehyde retrievals form the global ozone monitoring experiment. J. Geophys. Res. 106, 14539–14550. http://dx.doi.org/10.1029/2000JD900772.

Pany, T., Pesec, P., Stangl, G., 2001. Atmospheric GPS slant path delays and rays tracing through numerical weather models, a comparison. Phys. Chem. Earth Solid Earth Geod. 26, 183–188. http://dx.doi.org/10.1016/S1464-1895(01)00044-8.

Prasad, A.K., Singh, R.P., 2009. Validation of MODIS terra, AIRS, NCEP/DOE AMIP-II reanalysis-2, and AERONET sun photometer derived integrated precipitable water vapor using ground-based GPS receivers over India. J. Geophys. Res. Atmos. 114, 1–20. http://dx.doi.org/10.1029/2008JD011230.

Román, R., Antón, M., Cachorro, V.E., Loyola, D., Ortiz de Galisteo, J.P., de Frutos, A., Romero-Campos, P.M., 2015. Comparison of total water vapor column from GOME-2 on MetOp-A against ground-based GPS measurements at the Iberian Peninsula. Sci. Total. Environ. 533, 317–328. http://dx.doi.org/10.1016/j.scitotenv.2015.06.124.

Román, R., Bilbao, J., de Miguel, A., 2014. Uncertainty and variability in satellite-based water vapor column, aerosol optical depth and Angström exponent, and its effect on radiative transfer simulations in the Iberian Peninsula. Atmos. Environ. 89, 556–569. http://dx.doi.org/10.1016/j.atmosenv.2014.02.027.

Schrijver, H., Gloudemans, A.M.S., Aben, I., 2009. Water vapour total columns from SCIAMACHY spectra in the 2.36 μm window. Atmos. Meas. Tech. 2, 561–571. http://dx.doi.org/10.5194/amt-2-561-2009.

Schroedter-Homscheidt, M., Drews, A., Heise, S., 2008. Total water vapor column retrieval from MSG-SEVIRI split window measurements exploiting the daily cycle of land surface temperatures. Remote Sens. Environ. 112, 249–258. http://dx.doi.org/10.1016/j.rse.2007.05.006.

Torres, B., Cachorro, V.E., Toledano, C., Ortiz De Galisteo, J.P., Berjón, A., De Frutos, A.M., Bennouna, Y., Laulainen, N., 2010. Precipitable water vapor characterization in the Gulf of Cadiz region (southwestern Spain) based on sun photometer, GPS, and radiosonde data. J. Geophys. Res. Atmos. 115, 1–11. http://dx.doi.org/10.1029/2009JD012724.

Turner, D.D., Clough, S.A., Liljegren, J.C., Clothiaux, E.E., Cady-Pereira, K.E., Gaustad, K.L., 2007. Retrieving liquid water path and precipitable water vapor from the atmospheric radiation measurement (ARM) microwave radiometers. IEEE Transactions on Geoscience and Remote Sensing. vol. 45. pp. 3680–3689. http://dx.doi.org/10.1109/TGRS.2007.903703.

Turner, D.D., Ferrare, R.A., Heilman Brasseur, L.A., Feltz, W.F., Tooman, T.P., 2002. Automated retrievals of water vapor and aerosol profiles from an operational raman lidar. J. Atmos. Ocean. Technol. 19, 37–50. http://dx.doi.org/10.1175/1520-0426(2002)019¡0037:AROWVA¿2.0.CO;2.

Wang, H., Gonzalez Abad, G., Liu, X., Chance, K., 2016. Validation of OMI total column water vapor product. Atmos. Chem. Phys. Discuss. 181, 1–23. http://dx.doi.org/10.5194/acp-2016-181.

Wang, H., Liu, X., Chance, K., González Abad, G., Chan Miller, C., 2014. Water vapor retrieval from OMI visible spectra. Atmos. Meas. Tech. 7, 1901–1913. http://dx.doi.org/10.5194/amt-7-1901-2014.

Wilcoxon, F., 1946. Individual comparisons of grouped data by ranking methods. J. Econ. Entomol. 39, 269. http://dx.doi.org/10.2307/3001968.

Please cite this article as: J. Vaquero-Martínez et al., Validation of integrated water vapor from OMI satellite instrument against reference GPS data at the Iberian Peninsula, Science of the Total Environment (2016), http://dx.doi.org/10.1016/j.scitotenv.2016.12.032